



Applicability of Unmanned Aerial Systems for Leak Detection

Brendan Smith,
Garrett John and Brandon Stark
School of Engineering
University of California, Merced
Merced, CA 95343

Lance E. Christensen
Jet Propulsion Laboratory,
California Institute of Technology
Pasadena, California 91109
Email: lance.e.christensen@jpl.nasa.gov

YangQuan Chen
School of Engineering
University of California, Merced
Merced, CA 95343
Email: ychen53@ucmerced.edu

Abstract—In light of recent U.S. Federal Aviation Administration (FAA) notices, there is a surge in the research and development of the ‘micro’ class sUAS for commercial purposes. Natural gas production and distribution companies in particular are making an effort to develop aerial leak detection methods with sUAS. These efforts require a comprehensive evaluation of sUAS capabilities and the environmental disturbances introduced by the sUAS in order to accurately utilize data collected via onboard in situ methane gas sensors. Though many commercially available sUAS are on the market, the shape and arrangement of any system has significant impact on the aircraft’s ability to accurately sense gas leaks. This paper explores using a 3DRobotics Iris+ quadcopter for gas sensing, paying particular attention to propeller disturbances introduced by the sUAS. The paper defines certain operating conditions in which the influence of propellers can be ignored. These results can be used in gas leak applications by examining the overall airflow dynamics of a commercially available rotary sUAS.

Index Terms—methane leak detection, propeller wash, small-unmanned aerial systems, remote sensing

I. INTRODUCTION

Natural gas, primarily composed of methane, has become one of the major resources utilized in electricity and heat production. As a result, thousands of miles of gas distribution and transmission pipelines weave across the U.S., which require diligent monitoring for leaks and damaged lines [1],[2]. Several reliable methane detection methods exist and are currently utilized in the industry, such as portable active remote sensors (RMLD), cavity ringdown spectrometers [3], infrared methane gas imaging cameras [4]. These methods can be logistically difficult and costly to operate, providing inefficient spatial coverage due to the fact that they are operated at ground level along accessible pathways. Manned-aircraft methods also exist that can survey large spans of pipeline in a short amount of time, but these aerial systems are additionally high in operating cost and require skilled operators [5], [6], [7]. A potential solution to the inefficiency and cost of current methods is the application of small-unmanned aerial systems (sUASs).

In this scenario, the sUAS becomes a companion to the Leak Surveyor who’s occupation is to localize the methane leak. The sUAS effectively takes on role the co-Leak-Surveyor [8].

The U.S. Federal Aviation Administration (FAA) has published a notice to propose rule-making authorizing micro-sized sUASs, or μ UAS, for specific commercial operations, in which the ‘micro’ classification is a subcategory of sUAS limited to 2kg (4.4lbs) or less. Through this notice, many companies seek to employ sUAS for a wide range of applications. The implementation would authorize flights of sUAS under 25kg (55lbs) for specific commercial purposes, including pipeline surveillance. The purpose of this paper is to effectively explore the capabilities and implementation of sUAS for gas leak detection. Rotary aircraft are extremely disruptive to the air volume surrounding them in flight due to the effects caused by propeller wash. Propeller wash, also referred to as prop wash, is the phenomenon in which a spiral slipstream is formed by the rotation of the aircraft propeller blades [9]. This phenomenon is why implementation of *in-situ* gas sensors on vertical takeoff and landing (VTOL) aircraft is seemingly difficult. However, due to the availability, low cost, and ease of operation, rotary μ UAS are ideal for collecting large amounts of surveying data.

This paper focuses on the study and characterization of disruptive airflow caused by propeller-wash by a VTOL and its impact on a smoke plume. The tests conducted are designed to determine an optimal region of smoke sensing aboard an μ UAS through analysis. In Section II, an overall testing methodology is presented and discussed. Section III discusses the results of performing numerous tuft visualization and smoke visualization tests both statically and in flight. Finally, concluding remarks are presented in Section IV.

II. METHODOLOGY

In order to fully implement sUAS for leak detection applications, four tests were developed. These tests al-

low for a comprehensive evaluation of how the μ UAS indirectly interacts with the sensor under certain flight conditions. These tests will exhibit the regions of disruption and optimal sensor placement, surrounding and on the sUAS, respectively.

The IRIS+ platform, developed by 3D Robotics [10], satisfies necessary requirements such as payload capacity, power draw, weight and cost for current methane gas leak detection purposes. The Iris+ is classified as a μ UAS, which makes this platform ideal for larger scale implementation due to the potential for fewer limitations proposed by the FAA.

The following subsections detail the four comprehensive tests designed to fully evaluate the IRIS+ platform. These tests consist of the overall airflow disturbance of the μ UAS tests, smoke visualization tests for the characterization of rotor intake and outtake, flight tests with smoke sensing payloads and smoke plume reconstruction tests. Each testing group had tests performed in multiple iterations so as to validate the results found.

A. Evaluating the Overall Airflow Disturbance of the μ UAS

This testing section consisted of numerous tests in which the downwash shape and rotor outtake could be characterized. These tests relied on the extensive use of tuft visualization panels and a stabilized aircraft in order to reconstruct and model the shape of downwash produced by the μ UAS.

These tests allow for a model of the disturbance range of the μ UAS downwash to be measured and analyzed. It is necessary to quantify this range as it represents regions in which a methane gas sensor may not be mounted. This region is proven to be extremely disruptive to airflow beneath the aircraft and without proper understanding of this regions magnitude an optimal sensor placement can not be determined.

B. Smoke Visualization For Characterization Of Rotor Intake And Outtake

This test allowed the full effects of rotor intake and outtake to be visualized. The data collected characterizes the airflow, which helps determine the optimal placement for an *in-situ* methane gas sensor. In-flight characteristics such as pitch, roll and yaw were evaluated for total flight effects as well as identification of regions in which eddies formed or stagnant air was built up.

Testing these aspects is necessary for determining an optimal sensor location and simulating how the μ UAS will perform in varying flight conditions. Smoke visualization is first used to determine any probable locations for a methane gas sensor aboard the μ UAS and determining the true nature of the rotorcraft downwash shape.

C. Flight Test With Smoke Sensing Payload

Flight tests were determined to serve as a validation for the previous smoke visualization. An optical smoke sensor was used as a proxy for a methane gas sniffer. These tests investigated predetermined optimal regions in which the sensor appeared to be unaffected by prop wash. These tests were performed with an optical smoke sensor, flying into and above a smoke plume. Flight tests serve as a proof of concept of the aircrafts in-flight sensing capabilities and a validation of characteristics modeled through smoke visualization.

D. Smoke Plume Reconstruction

Smoke plume reconstruction is the single most important validation of μ UAS smoke sensing capabilities. This test compares sensor readings taken by a handheld smoke sensor versus a smoke sensor mounted aboard an μ UAS. Both sensor readings were used to reconstruct the plume and a comparison is made between the two data sets. This is necessary in proving the accuracy of the mounted sensor and proving that a plume can be accurately modeled and sensed by an μ UAS.

III. TESTING RESULTS

A. Overall Airflow Disturbance

Airflow disturbance tests relied on the use of an array of tuft visualization panels with 7.62cm (3in) long tufts. Tests were conducted both indoors and outdoors in order to characterize the overall downwash shape produced by the μ UAS. This also allowed for the determination of a minimum flight altitude at which air beneath the sUAS is no longer impacted by the rotors.

Initial outdoor tests proved the μ UAS demonstrates severe ground level disturbance at altitudes under 3m. Flights above 3m only demonstrated random bursts of disturbance at ground level. These random bursts were likely caused by changes in the μ UAS thrust for balancing and the flight controller of the aircraft.

Indoor tests were conducted in a more controlled setting. The μ UAS was tested at heights ranging from 0.75m to 2m in increments of 0.25m and at varying flight angles of pitch (0° to 20°) and roll (0° to 20°). These tests were performed by mounting the sUAS to a tripod and adjusting the altitude and flight angles accordingly.

Tests exhibited a rectangular region of influence beneath the aircraft that did not display significant lateral growth which can be seen in Figure 1. The region beneath the aircraft also changed shape and direction with a change in μ UAS orientation and flight angle.

The rectangular shape of the downwash region was an unexpected result. It cannot be concluded whether the occurrence of this rectangular shape was due to the shape of the tuft panel array or the layout of the IRIS+ air frame. In order to further characterize the shape and



Fig. 1. Ground level disruption at forward pitch, with indicated distance relative to ground

the effects of the rotors, more accurate tests need to be performed through smoke visualization.

B. Smoke Visualization Tests

Smoke Pathway visualization tests served to fully characterize the airflow effects of the μ UAS and determined the optimal region for mounting a methane gas sensing payload. The tests were conducted using a research grade smoke wand and optical smoke sensor as mock methane gas sniffer. Tests performed in this section allowed for a complete model of the total airflow disruption of the μ UAS to be constructed. This model relied on the comprehensive results of four specific procedures followed when performing smoke visualization. These procedures include:

- Lawn mower pattern
- Roll/Pitch/Yaw
- Propeller downwash
- Stagnant regions

The lawn mower procedure requires the smoke wand to be passed in front of the μ UAS as visualized in Figure 2. Where the black lines represent the path of the wand tip, with the arrowheads indicating the direction of travel. The path is superimposed over an image of the IRIS+ in order to demonstrate the initial point of the smoke source relative to the vertical and lateral position of the aircraft.

This pattern allows for a complete evaluation of the airflow around the entire μ UAS to be made. The data analysis performed following these tests effectively confirms that characterization of the airflow past the quad-rotor is possible and identification of all disruptive regions can be extracted. The most important observation from these tests is that the airflow is directed towards the body of the μ UAS. Figure 3 demonstrates the flow of air entering the region of influence surrounding the μ UAV caused by the propellers. The region of influence begins at the purple dashed line, where a gradual slope downwards towards the aircraft begins. A second threshold is passed at the dashed green line, where the airflow begins to rapidly approach the trailing propellers. This



Fig. 2. Illustration of lawn mower pathway performed with a smoke wand

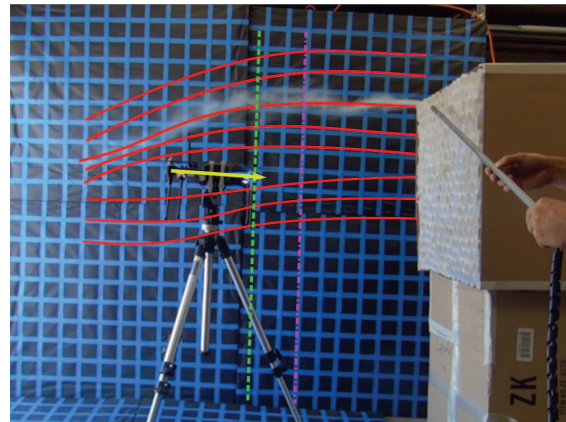


Fig. 3. Composite image of smoke pathways on the vertical axis

phenomenon exhibits that the airflow beneath the aircraft is forced downward by turbulent propeller wash. Airflow above the aircraft is observed to experience disruptive turbulence from propeller intake.

Airflow around the μ UAS is characterized further by adjusting the angles of roll, pitch, and yaw within the operation limits of the sUAS. The smoke pathways at each angle could then be observed and traced from the video footage recordings taken throughout experimentation. Alterations to angles of flight allow the characterization for the sUAS airflow to be more realistic and provide further data for how the sUAS may operate in the field, while still under the restrictions of simulated flight conditions. This procedure further characterized the effects of flight angles and proved their large impact on rotor intake and outtake. It concluded any changes in yaw only increased airflow disruption about the sUAS.

Further examination of the propeller downwash val-



Fig. 4. Cylindrical downwash produced by propeller outtake

identates testing performed for the overall airflow disturbance of the sUAS. Using smoke visualization allows the effective volumes of propeller outtake to be further quantified and evaluated. This procedure brought about the realization of a more cylindrical shaped outtake when smoke passes directly into the propellers as exhibited in Figure 4.

The propeller outtake also displayed extreme turbulence and cyclonic behavior. In addition, Propeller outtake completely dispersed any smoke that was built up beneath the sUAS, which is not ideal for sensing airborne substances including methane gas.

The last procedure utilizes complete airflow characterization in the identification of stagnant air regions. A stagnant air region is defined as any region where airflow is visibly free of the effects of propeller intake and outtake. These regions would then be evaluated as the most optimal locations for the sensor placement. This procedure concluded the identification of one major stagnant airflow region in the front of the sUAS body. A comparison between the stagnant region and a non-stagnant region can be seen in Figure 5 and 6. This region displayed virtually no effects from propeller wash. With the identification of this stagnant airflow region the importance of the IRIS+ unique air frame was realized. The IRIS+ air frame places the front rotors 3.175cm (1.25in) further apart in comparison to the rear rotors. This provided an ample region of airflow just between the rotors and created this stagnant region of airflow.

Analysis of previous video footage as well as of the structure of the sUAS allowed for exact dimensions of the region to be calculated at 20.32cm (8in) just under the body of the aircraft centered between the front two rotors (Figure 7).

The region was determined to drastically decrease at varying angles of wind direction. When the aircraft is yawed at a 45° angle from the parallel path of the wind source, then the region decreases to a width of 14.22cm (5.6in).

With the combined characterizations, a composite

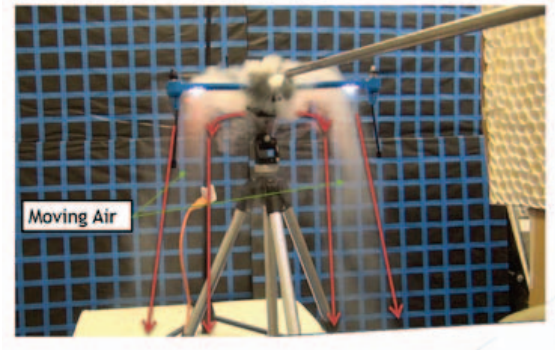


Fig. 5. Visualization of the cyclonic down-wash from rotors of the sUAS

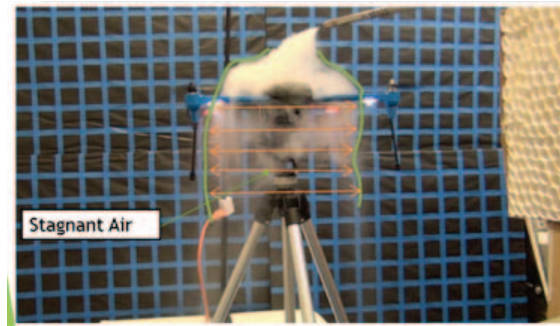


Fig. 6. Identification of stagnant region beneath the sUAS

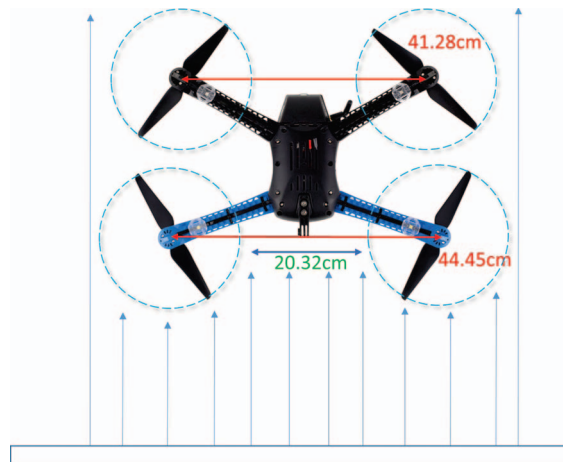


Fig. 7. Calculated region of airflow

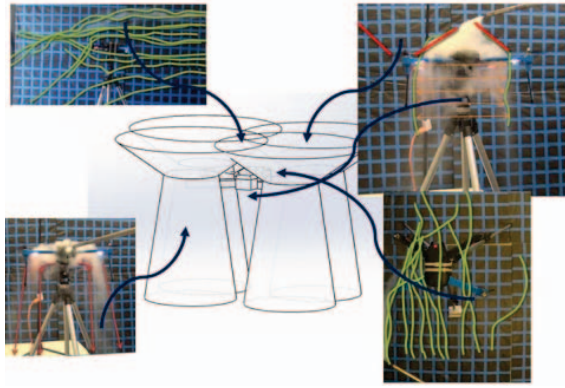


Fig. 8. Composite visual representation of regions of airflow disruption

visual representation of the entire influence region of the rotors is compiled. Figure 8 shows how each testing result contributed to produce an entire influence region model.

These tests proved conclusive data about the fluid dynamics of a rotary sUAS. Each test provided significant evidence that determined the optimal placement of a methane sensing payload.

The lawn mower testing procedure identified the nature of the airflow around the sUAS body to be minimally disrupted by the rotor effects. This suggests that the optimal regions for sensor placement are located on the body of the aircraft where flow is observed to be more laminar.

The changes in angles of roll, pitch, and yaw were tested and produced large variations in airflow regions effected by sUAS intake and outtake. This result is hypothesized to be caused by the angle of the propeller blades and the increased thrust of the flight controller for stabilization. This suggests that inflight aircraft orientation is a key consideration for airborne methane gas sensing with any rotary sUAS.

The propeller downwash resulted to be extremely turbulent and cyclonic. It is assumed that this turbulence is due to the propeller angles and its tendency to deflect the air. This further reaffirms the assumption that any sensing done beneath the rotors will be inaccurate and subject to large volumes of turbulent air flow which is non-ideal for methane gas leak detection.

This specifically resulted in the identification of a stagnant air region between the two front rotors of the sUAS. It was concluded that the geometry of this region is due to the unique air frame structure of the IRIS+. This suggested an important correlation between the rotor separation distance and the size of stagnant airflow regions of an sUAS.

C. Flight Tests

Flight tests served as a validation of the payload sensing capabilities and the characterization of airflow dynamics about the sUAS observed in previous testing. The tests consist of flying into and above smoke plume sources to visualize the disruptive nature of the aircraft in flight as well as validating the dimensions of the undisturbed air flow region.

1) *Test 1: Flight into the Plume:* This test was designed to test the capabilities of smoke sensing as well as further characterization. Ultimately, it serves as a proof of concept of inflight smoke sensing. The UAS is flown directly into a plume of smoke to ensure that the smoke is passing through the minimally disturbed airflow region and readings of the smoke sensing payload are monitored and recorded.

The test exhibits the disruptive air effects of the UAS on the plume source evaluated in previous tests. The smoke sensing payload was implemented here to prove the existence and accuracy of the airflow region previously defined.

Readings from the smoke sensing payload were sent to the ground control station via telemetry link and compared to video footage for accuracy. The flight pattern of the sUAS could be described as jousting into the plume. This method was utilized in order to provide substantial airflow beneath the μ UAS for optical sensor readings to be taken. The results from this test are summarized as follows:

- the existence of an airflow region was confirmed beneath the aircraft;
- smoke readings can be taken accurately in flight;
- smoke sensing is directional and must be done by flying into the wind and against the direction of the plume;
- proficient airflow of at least $2 \frac{m}{s}$ needs to be present to sense in this region;
- and jousting flight pattern was the most effective way to produce accurate readings.

This test brought about the realization of minimum airflow of $2 \frac{m}{s}$ through the airflow region in order to sense smoke accurately. Readings within the uninhibited airflow region were unpredictable and random when a wind speed of at least $2 \frac{m}{s}$ was not achieved. This could be achieved by a combination of wind speed and ground speed of the sUAS, but needed to equate to at least $2 \frac{m}{s}$ in order to provide accurate readings.

2) *Test 2: Flight over the Plume:* This test characterized the plume flow in which the point of origin is below the flight altitude of the aircraft and examined the ability of the UAS to loiter over a smoke source and take possible readings. In addition, the test served as a vital tool in determining the placement of a smoke or

methane sensing payload. This method would be ideal for smoke sensing if the rotor wash were only minimally disruptive and smoke was not largely displaced.

This test required a large cloud or plume of smoke to be produced to track total displacement beneath the aircraft. Throughout the testing, video recordings were taken as visual evidence to quantify total smoke displacement. Footage is processed and examined to see the effects of loitering or hovering the aircraft.

The results of these tests are summarized as follows:

- smoke is largely displaced by the downwash of the sUAS;
- rotor wash is extremely disruptive to a plume source beneath the sUAS;
- loitering or hovering is not an effective means for accurately sensing a plume;
- almost all smoke was displaced by the sUAS in both cloud and plume settings;
- an increased dispersion rate of the smoke beneath the aircraft was observed.

These results completely contradict any ability for the aircraft to operate and hover above a plume source. This experiment was restricted by the amount of smoke produced due to the output of a single smoke wand. A larger plume source may produce additional information, but the disruptive nature beneath the aircraft will still be overwhelming.

D. Validation of Undisturbed Airflow

This test validates the calculation done to determine the dimensions of the airflow region between the front propellers. The smoke sensor was mounted in eight different positions within the 20.32cm (8in) region and tested with a smoke plume source. The smoke sensor was also once again mounted directly beneath the rotors to ensure no sensing occurred. The results of this test are summarized as follows:

- smoke sensor takes accurate readings across entire 20.32cm (8in) region;
- just outside of the 20.32cm (8in) region readings are still able to be taken but subject to non-ideal airflow effects;
- any sensor mounted directly beneath the props pick up no readings.

E. Smoke Plume Reconstruction

This test served as a comparison between the capabilities of a handheld sensor versus a sensor mounted to the aircraft in simulated flight conditions. The readings of the sensor mounted to the aircraft validated its sensing capabilities and its accuracy when mounted in the 20.32cm (8in) airflow region. Figure 10 and 11 display the readings taken with the handheld optical smoke sensor. This produced a control data set that is



Fig. 9. Diagram conveying valid smoke sensing region

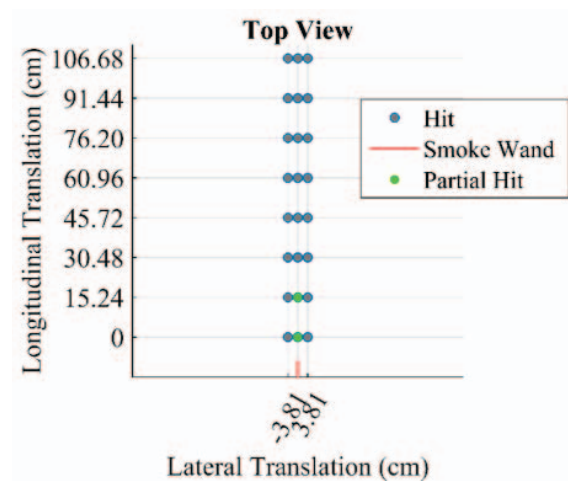


Fig. 10. Longitudinal vs. lateral translation points from a 3D reconstruction profile of plume with handheld sensor without μ UAS, top view

uninhibited by the disruptive nature of the aircraft and any aerodynamics that may influence air flow.

Data was then received using the same optical smoke sensor mounted to μ UAS under simulated flight conditions. This way the smoke sensing region of the μ UAS could be evaluated for accuracy. This data can be seen in Figure 12 and 13.

A comparison between the data sets displayed in the two side views (Figure 11 and 12) and top views (Figure 10 and 13) is then made to evaluate the number of similar readings. Readings were observed at varying location up to a distance of approximately 120cm (48in) from the wind tunnel and both partial and consistent hits

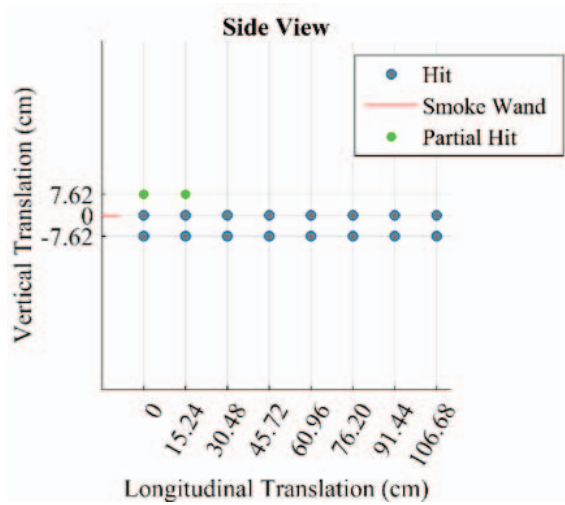


Fig. 11. Vertical vs. longitudinal translation points from a 3D reconstruction profile of plume with handheld sensor without μ UAS, side view

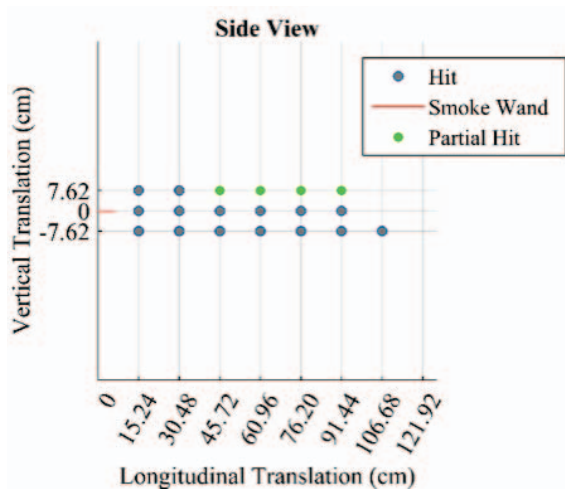


Fig. 12. Vertical vs. longitudinal translation points from a 3D reconstruction profile of plume with handheld sensor on μ UAS, side view

were recorded. Partial hits were quantified as fluctuating readings while consistent hits provided a full reading during the sensing period.

The results from this test reaffirmed the smoke sensing capabilities within the uninhibited airflow region. These findings concluded an 82% similarity between the readings of the handheld smoke sensor and the mounted smoke sensor.

- Reaffirmed accurate sensing capabilities within uninhibited airflow region
- 82% similarity between the handheld and mounted sensor
- 18% error is spatially patterned within the data set as distance from the tunnel increases

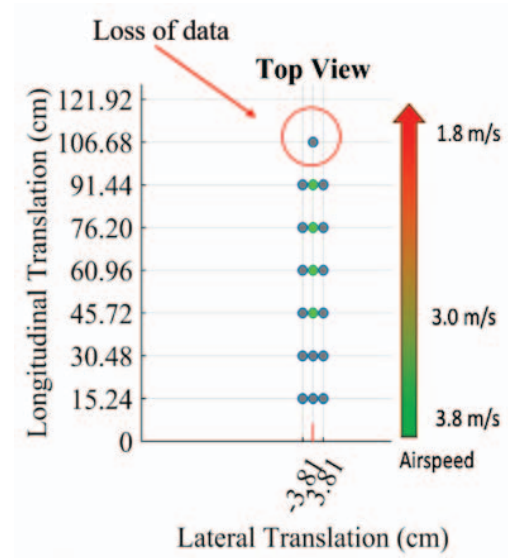


Fig. 13. Measured decrease in wind speed comparison to loss of data UAS readings

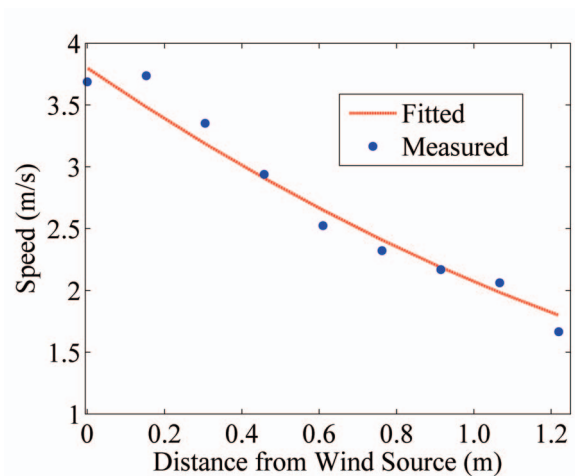


Fig. 14. Speed vs. Distance of constructed wind tunnel in all experimentation

This test may have been easily influenced by a number of variables resulting in an 18% error which are summarized here:

- ambient wind effects from indoor A/C,
- non-uniform airflow of the wind tunnel.

Figure 13 shows a loss of data when distance from the plume increases. The wind speed also decreases to below $2 \frac{m}{s}$ which is necessary for sensing. This most likely caused the 18% error in readings taken aboard the sUAS.

IV. CONCLUSIONS

In conclusion, the project effectively explored the capabilities and implementations of an μ UAS for methane gas leak detection. Testing results concluded sensing

capabilities of any rotary aircraft is highly dependent on μ UAS air frame design. Even though the tests performed were successful, much progress needs to be made to fully implement this product for methane detection aboard an μ UAS.

Numerous testing methodologies were developed and completed to characterize the propeller wash and determine an optimal placement of a methane gas leak detection payload. Tests were completed utilizing multiple air-flow visualization techniques and many iterations were completed. The results of each test were compiled into a comprehensive list to allow for total characterization of the UAS airflow. A similar procedure and compilation of results should be found and applied to any vertical take-off and landing (VTOL) or rotary aircraft employed for methane gas leak detection. These results focus on the total disruptive nature of the μ UAS and the identification of specific regions that are void of these disruptions. The most important conclusion from these tests was the value in a wider air frame for a rotary aircraft. The unique wider air frame of the Iris+ allowed more airflow between the front rotor wash, which allowed for a larger region of uninhibited airflow.

In order to validate airflow characterization observations and prove the ability of a rotary aircraft to sense sensitive air volumes accurately; a mock up payload needed to be constructed. A simple digital optical dust sensor served as an adequate payload to determine optimal placement for the methane gas sensor. The optical dust sensor was placed on the IRIS+ in various locations and tested with the smoke generator. These tests suggested the best possible location to be a 20.32cm (8in) region just under the front of the body of the aircraft. The optimal position for smoke sensor placement is in the air flow region of the Iris+. It was also concluded that a specific flight pattern of jousting into a plume would be required to achieve a necessary airflow of $2\frac{m}{s}$ passed the sensor.

While there exists a region of undisturbed air from which methane may be sensed, proper sensing can be accomplished only under certain conditions. To pass methane gas into the region undisturbed by propeller wash, a steady airflow velocity, estimated above $2\frac{m}{s}$, is necessary. Below this airflow speed, sensor readings were unreliable, and no air particles were visible within the window. The air disturbed by the propeller wash of the μ UAS is significant, and during test flights, dispersed any particles as far as 5m.

The tests performed were able to characterize the propeller wash accurately and effectively. In addition, it provided a standard procedure for characterizing effective sensing region for any VTOL or rotary aircraft. To test this methodology again, future testing considerations need to be addressed. The overall development of testing

infrastructure can be greatly improved to produce the most accurate testing results. A larger smoke plume may also be necessary in fully characterizing smoke sensing capabilities during flight tests. Further development of these infrastructures will drastically improve testing results. The smoke sensor may also benefit from testing plume reconstruction at distances greater than 122cm (48in) away from the plume source. These efforts will allow further conclusions to be made and more accurate data can be produced.

ACKNOWLEDGMENT

This work was funded in part by Pacific Gas & Electric (PG&E), with additional guidance and support from François Rongere and Gerry Bong. Special thanks to Nathaly Navarette for her dedication to the success of this project.

REFERENCES

- [1] J. Davalle. (2011, May) Gas detection through the ages. [Online]. Available: <http://ehstoday.com>
- [2] M. W. Heath III, "Methane leak detection and measurement technologies," in *Turkmenistan Symposium on Gas Systems Management: Methane Mitigation*, April 2010.
- [3] E. Crosson, "A cavity ring-down analyzer for measuring atmospheric levels of methane, carbon dioxide, and water vapor," *Applied Physics B*, vol. 92, no. 3, pp. 403–408, 2008. [Online]. Available: <http://dx.doi.org/10.1007/s00340-008-3135-y>
- [4] C. Massie, G. Stewart, G. McGregor, and J. R. Gilchrist, "Design of a portable optical sensor for methane gas detection," *Sensors and Actuators B: Chemical*, vol. 113, no. 2, pp. 830–836, 2 2006. [Online]. Available: <http://www.sciencedirect.com/science/article/pii/S0925400505003539>
- [5] A. Trégourès, A. Beneito, P. Berne, M. A. Gonze, J. C. Sabroux, D. Savanne, Z. Pokryszka, C. Tauziède, P. Cellier, P. Laville, R. Milward, A. Arnaud, F. Levy, and R. Burkhalter, "Comparison of seven methods for measuring methane flux at a municipal solid waste landfill site," *Waste Management and Research*, vol. 17, no. 6, pp. 453–458, 1999. [Online]. Available: <http://dx.doi.org/10.1034/j.1399-3070.1999.00065.x>
- [6] R. T. Wainner, M. B. Frish, B. D. Green, M. C. Laderer, M. G. Allen, and J. R. Morency, *High Altitude Aerial Natural Gas Leak Detection System*, Dec 2006. [Online]. Available: <http://www.osti.gov/scitech/servlets/purl/921001>
- [7] H. M. Kalayeh, G. R. Paz-Pujalt, and J. P. Spoonhower, "System and method for remote quantitative detection of fluid leaks from a natural gas or oil pipeline," U.S. Patent 6822742 B1, Tech. Rep., November 2004.
- [8] "The era of robotic environmental co-journalists," in *Symp. on Groundtruth and Airwaves: Sensor Networks and Emerging Technology for Environmental Journalism, Center for Information Research in the Interest of Society*. Banatao Auditorium, Sutardja Dai Hall, University of California, Berkeley, April 2015. [Online]. Available: https://youtu.be/_eWkwD9CGrQ
- [9] D. Yeo, E. Shrestha, D. A. Paley, and E. M. Atkins, *An Empirical Model of Rotorcraft UAV Downwash for Disturbance Localization and Avoidance*. American Institute of Aeronautics and Astronautics, 2015/10/31 2015. [Online]. Available: <http://dx.doi.org/10.2514/6.2015-1685>
- [10] 3D Robotics. (2015). [Online]. Available: <http://3drobotics.com>